J Supercond Nov Magn (2015) 28:1471–1476
DOI 10.1007/s10948-014-2921-5

ORIGINAL PAPER

Enhanced Transport Critical Current Density in Ag-Sheathed $(Bi_{1.6}Pb_{0.4})Sr_2Ca_2Cu_3O_y$ Superconductor Tapes with Different Nano-Sized Co_3O_4 Addition

A. N. Jannah · H. Abdullah · R. Abd-Shukor

Received: 3 April 2014 / Accepted: 28 November 2014 / Published online: 16 December 2014

Abstract Ag sheathed $(Bi_{1.6}Pb_{0.4})Sr_2Ca_2Cu_3O_y(Co_3O_4)_x$ superconductor tapes with addition of Co_3O_4 nanoparticles (with size 30 and 50) were fabricated using the powder-in-tube (PIT) method. The structure and microstructure were studied along with critical temperature (T_c) and transport critical current density (J_c). The nanoparticle added tapes showed a higher J_c value compared with the non-added tapes. The 30-nm Co_3O_4 added tapes showed a higher J_c value compared with the 50 nm Co_3O_4 added tapes. This study showed that Co_3O_4 nanoparticles could act as effective pinning centers leading to enhancement of J_c in the Bi-2223/Ag sheathed tapes. The addition of smaller Co_3O_4 nanoparticles (30 nm) results in stronger pinning. The full vortex magnetic energy due to addition of Co_3O_4 magnetic nanoparticles led to the enhancement of J_c.

Keywords Co-precipitation · Critical current density · Critical temperature · Nanoparticles

1 Introduction

Large-scale applications of high-critical temperature (T_c) superconductors at liquid nitrogen temperature under magnetic fields require high transport critical current density. The flux pinning capability is one of the basic parameters that is important for the application of superconductors. In order to enhance the flux pinning properties and improve the transport current density, many attempts have been made by introducing artificial defects of nanometer size as possible pinning centers [1–6]. The improvement in transport critical current density (J_c) can be obtained by introducing an efficient pinning center with size that matches the coherence length. Magnetic nanoparticles have been suggested as effective pinning centers [7, 8]. The use of magnetic nanoparticles with various shapes such as nanorod has been suggested to increase the pinning potential and thus enhance J_c [9].

The two important characteristic lengths in superconductors are the coherence length (ξ) and penetration depth (λ). Generally, the critical current density will increase when the size of magnetic particles is increased, and L is larger than ξ but smaller than λ [10]. In another report however, pinning is expected to be optimized when the size of the defects approaches the coherence length. The coherence length of $Bi_2Sr_2Ca_2Cu_3O_{10}$ is 2.9 nm [11] and penetration depth is in the range of 60–1000 nm. Provided that the particle size is carefully controlled i.e. between 2.9 and 60 nm and the dopant level is kept below a critical threshold, the addition of nanoparticles may improve the flux pinning [9, 12].

The J_c of the nano-sized Fe_3O_4 added tapes is 5130 A/cm^2 at 77 K and 23130 A/cm^2 at 30 K in zero fields. Fe_3O_4 can act as an effective flux pinning center leading to enhancement of J_c in the bulk as well as the tape form [13]. The J_c (77 K) of the 6-nm ZnOadded sample was 46 times larger than that of the non-ZnOadded sample [14]. In nano-sized MgOadded tapes, the temperature and magnetic field dependence of J_c exhibited significant enhancement compared with the non-added tapes [15]. The nanoparticle with size closer to the coherence length was suggested to be more effective in enhancing J_c [13–15].

Most studies on enhancing J_c only used one size nanoparticles. It is interesting to investigate the effect of

A. N. Jannah · R. Abd-Shukor (✉)
School of Applied Physics, Universiti Kebangsaan Malaysia, 43600 Bangi, Selangor, Malaysia
e-mail: ras@ukm.edu.my

H. Abdullah
Department of Electrical, Electronic and Systems Engineering, Faculty of Engineering and the Built Environment, Universiti Kebangsaan Malaysia, 43600 Bangi, Selangor, Malaysia

different sized magnetic nanoparticles on the transport current properties of the Bi-2223 superconductors. In this work, Co_3O_4 magnetic nanoparticles with an average size of 30 and 50 nm were added into $Bi_{1.6}Pb_{0.4}Sr_2Ca_2Cu_3O_{10}$ (Bi-2223) Ag-sheathed tapes. These sizes were chosen because according to a previous theoretical study [9], when the magnetic nanoparticle size is larger than the coherence length but smaller than the penetration depth, enhanced flux pinning is expected. Nano-Co_3O_4 is superparamagnetic above 45 K, ferromagnetic between 25 and 45 K, and antiferromagnetic below the transition temperature of 27 K which is less than that of the bulk value $T_N = 33$ K [16]. The effect of these nanoparticles on the microstructure and the electrical transport properties of Bi-2223/Ag tapes are reported.

2 Experimental Details

Superconductor powders with nominal starting composition $(Bi_{1.6}Pb_{0.4})Sr_2Ca_2Cu_3O_y(Co_3O_4)_x$ (x = 0–0.05 *wt* %) were synthesized using the co-precipitation method. The average particle size of Co_3O_4 was 30 and 50 nm. Using the results from the polycrystalline samples that showed that J_c was optimized with 0.02 wt % in 30-nm Co_3O_4added pellets and 0.01 wt % in 50-nm Co_3O_4added pellets, Ag-sheathed superconductor tapes were fabricated using the powder-in-tube method. The $(Bi_{1.6}Pb_{0.4})Sr_2Ca_2Cu_3O_{10}$ powders were added with 0.02 wt % Co_3O_4 (30 nm) and 0.01 wt % Co_3O_4 (50 nm) nanoparticles before being packed into a Ag tube with an outer diameter of 6.03 mm and an inner diameter of 4.43 mm. The tube was drawn into a 1 mm wire by extrusion process and then pressed into tape of 0.30 mm in thickness and 1.53 mm in width. The tapes were then sintered at 845° C for 50 h and cut into 3 cm sections for J_c measurements.

The electrical resistance–temperature measurements were carried out using the four-point probe technique in conjunction with a CTI cryogenics closed-cycle refrigerator (model 22). The four-point probe method using the 1-μV/cm criterion was used to measure the transport critical current density (J_c) between 30 and 77 K. J_c was also measured in a magnetic field of 0–0.75 T at 77 K.

The phase was determined using the X-ray diffraction (XRD) method by employing a Bruker D8 Advance diffractometer. The size of Co_3O_4 was determined using a Philips transmission electron microscope (TEM) (model CM12).

3 Results and Discussion

The average size of Co_3O_4 particles calculated from the TEM micrographs was 30 ± 4 and 50 ± 4 nm. Figure 1 shows the TEM micrograph of the 30-nm Co_3O_4 particles. Figure 2 shows the XRD patterns of the tapes with $x = 0$ *wt* %, $x = 0.02$ *wt* % of Co_3O_4 (30 nm), and $x = 0.01$ *wt* % of Co_3O_4 (50 nm). X-ray diffraction patterns show that the Bi-2223 is the major phase, while the Bi-2212 is the minor phase in all tapes.

Figure 3 shows the microstructure of the $x = 0$ wt %, $x = 0.02$ wt % of Co_3O_4 (30 nm), and $x = 0.01$ wt % of Co_3O_4 (50 nm) tapes. Plate-like grains are observed in the non-added sample that is normally observed in the Bi-based system. The non-added sample showed a larger grain size than the sample with nano-Co_3O_4. The grain morphology of all the added samples was almost similar, except for minor variations in texture and porosity.

Figures 4 and 5 shows the critical current density versus Co_3O_4 content in polycrystalline $Bi_{1.6}Pb_{0.4}Sr_2Ca_2Cu_3O_{10}$ at 30 and 77 K. The highest J_c was observed in the $x = 0.02$ wt % Co_3O_4 (30 nm) sample and in the $x = 0.01$ wt % Co_3O_4 (50 nm) sample [17]. Figure 6 shows the temperature dependence of J_c in zero magnetic fields for $x = 0$ wt %, $x = 0.02$ wt % of Co_3O_4 (30 nm), and $x = 0.01$ wt % of Co_3O_4 (50 nm)-added tapes. Table 1 shows the J_c of $Bi_{1.6}Pb_{0.4}Sr_2Ca_2Cu_3O_{10}$ tapes with and without the addition of Co_3O_4 nanoparticles at 30 and 77 K in zero fields. J_c for the added samples was higher than that for the non-added tape. The highest J_c at 30 K (22800 A/cm^2) and 77 K (6840 A/cm^2) was shown by the sample with Co_3O_4 (30 nm). This result showed that Co_3O_4 nanoparticles enhanced the transport critical current density in the bulk and tape samples. In the intermediate temperature region (between 35 and 55 K), the J_c of the 50-nm Co_3O_4-added tapes was higher than that of the 30-nm Co_3O_4-added tapes. This indicated the possible different flux pinning mechanisms in this region for the two tapes.

The magnetic field dependence of the critical current density at 77 K with fields parallel and perpendicular to the tapes' surface is shown in Fig. 7. The J_c decreased when the magnetic field was applied parallel to the surface of the tape due to the strong anisotropy of Bi-2223. The J_c of tape with $x = 0.01$ wt % of Co_3O_4 (50 nm) tape decreased faster than that with $x = 0.02$ wt % of Co_3O_4 (30 nm) tape. The nano-sized particles introduced into the granular networks are believed to act as possible pinning centers, and this improved the microstructure and strengthens the weak links between grains.

In conclusion, the effect of nano-sized Co_3O_4 addition on flux pinning capability of $(Bi_{1.6}Pb_{0.4})Sr_2Ca_2Cu_3O_{10}$ tape was investigated. The highest J_c in the tapes was observed in the sample with $x = 0.02$ wt % Co_3O_4 (30 nm). All the nanoparticleadded samples showed a higher J_c value compared with the non-added samples. This study showed that the magnetic nanoparticles could act as effective pinning centers leading to enhancement of J_c. The preparation

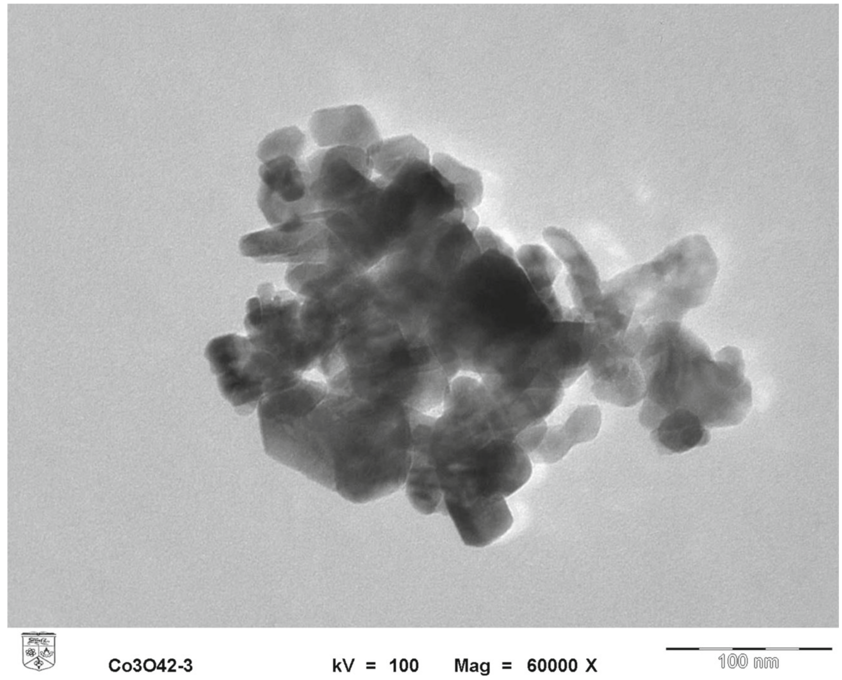

Fig. 1 TEM micrograph of Co_3O_4 showing an average grain size of 30 nm

method can be further optimized to improve the electrical transport properties. The flux line network and the magnetic texture can interact effectively if their characteristic scales have the same order of magnitude. Generally, when the size of a pinning center is larger than ξgut smaller than λ, the critical current density will increase. The average size of the Co_3O_4 used in this study is L =∼30–50 nm, and this satisfies the requirement $\xi < L < \lambda$ for a frozen flux superconductor, which is likely an explanation for the enhanced J_c in the system. The full vortex magnetic energy from the

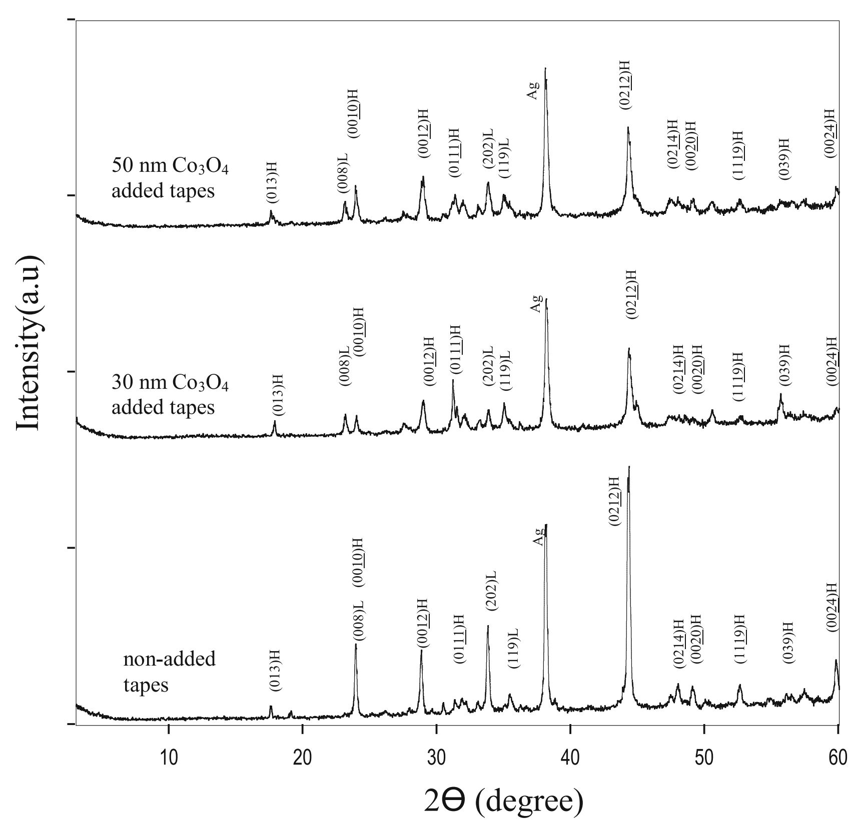

Fig. 2 XRD patterns of the tape sample for $x = 0$ wt %, $x = 0.02$ wt % of Co_3O_4 (30 nm), and $x = 0.01$ wt % of Co_3O_4 (50 nm). H denotes the high-T_c phase (Bi-2223), and L denotes the low-T_c phase (Bi-2212)

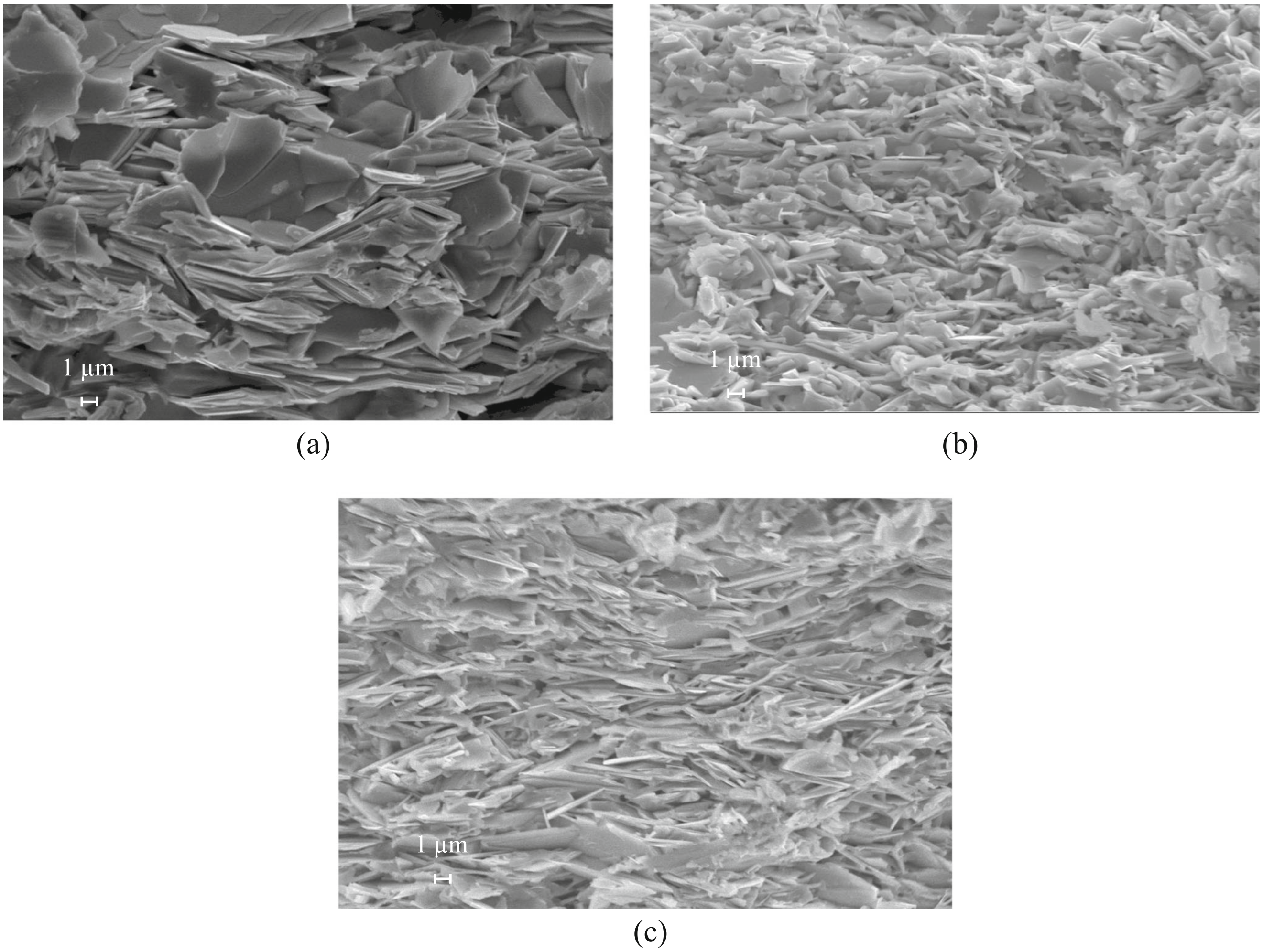

Fig. 3 SEM micrographs of the tape sample for **a** $x = 0$ wt %, **b** $x = 0.02$ wt % of Co_3O_4 (30 nm), and **c** $x = 0.01$ wt % of Co_3O_4 (50 nm)

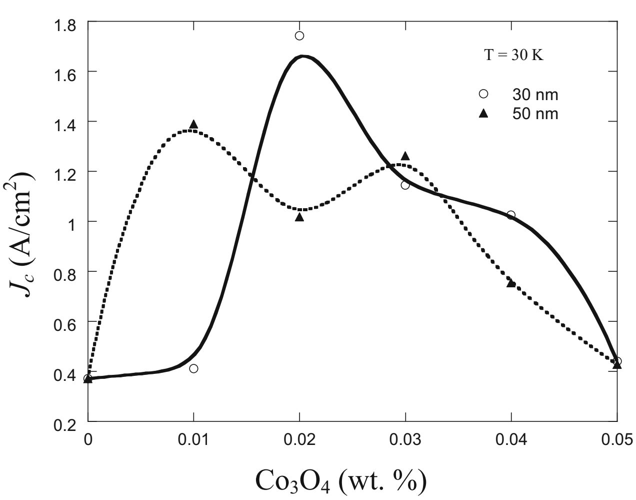

Fig. 4 Critical current density (J_c) versus Co_3O_4 content in $Bi_{1.6}Pb_{0.4}Sr_2Ca_2Cu_3O_{10}$ pellets at 30 K

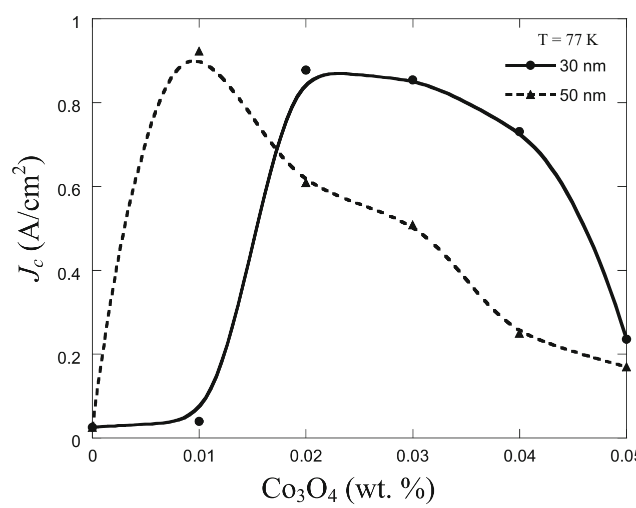

Fig. 5 Critical current density (J_c) versus Co_3O_4 content in $Bi_{1.6}Pb_{0.4}Sr_2Ca_2Cu_3O_{10}$ pellets at 77 K

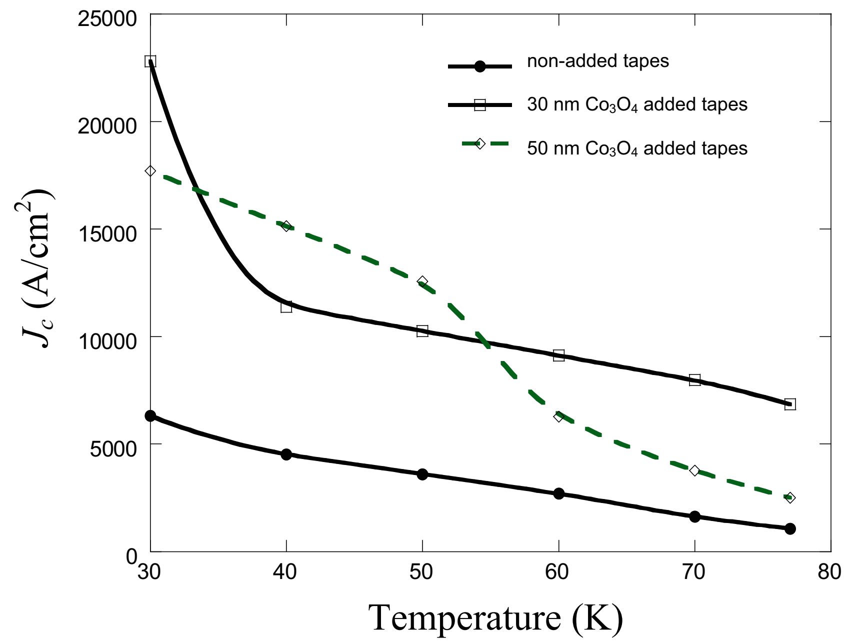

Fig. 6 Temperature dependence of J_c in zero magnetic fields for the tape samples for $x = 0$ wt %, $x = 0.02$ wt % of Co_3O_4 (30 nm), and $x = 0.01$ wt % of Co_3O_4 (50 nm)

Table 1 Critical current density (J_c) of $Bi_{1.6}Pb_{0.4}Sr_2Ca_2Cu_3O_{10}$ tapes with and without the addition of the Co_3O_4 nanoparticles at 30 and 77 K in zero fields

Composition	J_c (30 K) (A/cm^2)	J_c (77 K) (A/cm^2)
$Bi_{1.6}Pb_{0.4}Sr_2Ca_2Cu_3O_{10}$	6320	1080
$(Bi_{1.6}Pb_{0.4})Sr_2Ca_2Cu_3O_y(Co_3O_4)_{0.02}$(30 nm)	22800	6840
$(Bi_{1.6}Pb_{0.4})Sr_2Ca_2Cu_3O_y(Co_3O_4)_{0.01}$(50 nm)	17700	2510

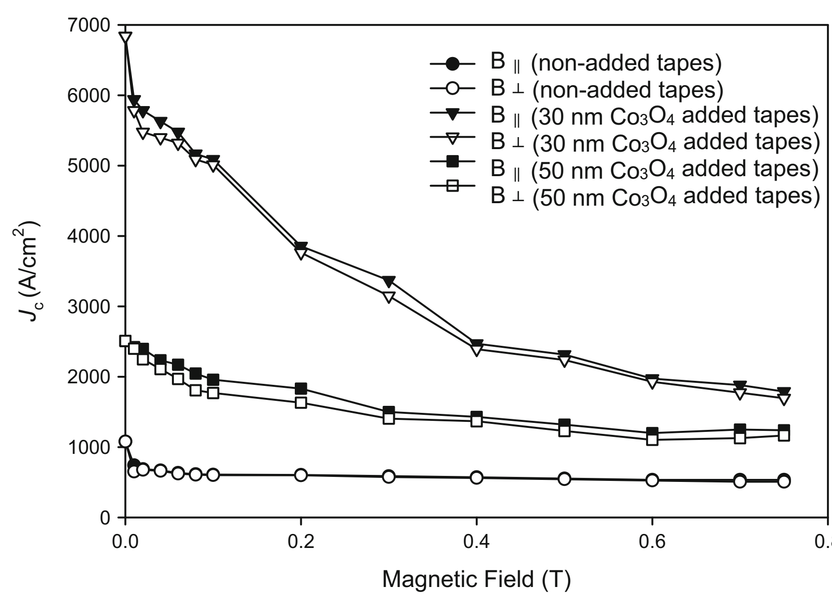

Fig. 7 J_c dependence on magnetic field applied both parallel and perpendicular to the tape surface, at 77 K, for the tape samples for $x = 0$ wt %, $x = 0.02$ wt % of Co_3O_4 (30 nm), and $x = 0.01$ wt % of Co_3O_4 (50 nm)

addition of Co_3O_4 magnetic nanoparticles played an important role in enhancing J_c in $Bi_{1.6}Pb_{0.4}Sr_2Ca_2Cu_3O_{10}$/Ag apes.

Acknowledgments This research was supported by the Ministry of Education, Malaysia, under grant no. FRGS/2/2013/SG02/UKM/01/1 and the Universiti Kebangsaan Malaysia under grant no. UKM-DIP-2012-032.

References

1. Jiang, J., Chai, X.Y., Polyanskii, A.A., Schwartzkopf, L.A., Larbalestier, D.C., Parrella, R.D., Li, Q., Rupich, M.W., Riley Jr., G.N.: Supercond. Sci. Technol. **14**, 548 (2001)
2. Pu, M.H., Song, W.H., Zhao, B., Wu, X.C., Hu, T., Sun, Y.P., Du, J.J.: Supercond. Sci. Technol. **14**, 305 (2001)
3. Çelebi, S., Düzgün, I.: Supercond. Sci. Technol. **22**, 034018 (2009)
4. Abd-Shukor, R., Yahya, S.Y., Jumali, M.H., Hamadneh, I., Halim, S.A.: J. Phys. : Conf. Series **43**, 71 (2006)
5. Abd-Shukor, R., Awang Kechik, M.M., Halim, S.A.: J. Phys: Conf. Series **97**, 012050 (2008)
6. Kusevic, I., Simundic, P., Babic, E., Ionescu, M., Liu, H.K., Dou, S.X.: Solid State Comm. **100**, 187 (1996)
7. Yang, Z.Q., Su, X.D., Qiao, G.W., Guo, Y.C., Dou, S.X., de Boer, F.R.: Physica C **325**, 136 (1999)
8. Ghattas, A., Annabi, M., Zouaoui, M., Ben Azzouz, F., Ben Salem, M.: Physica C **468**, 31 (2008)
9. Lyuksyutov, I.F., Naugle, D.G.: Mod. Phys. Lett. **13**, 491 (1999)
10. Mousavi Ghahfarokhi, S.E., ZargarShoushtari, M.: Physica B **405**, 4643 (2010)
11. Gul, I.H., Amin, F., Abbasi, A.Z., Anis-ur-Rehman, M., Maqsood, A.: Physica C **449**, 139 (2006)
12. Albiss, B.A., Obaidat, I.M., Gharaibeh, M., Ghamlouche, H., Obeidat, S.M.: Solid State Comm. **150**, 1542 (2010)
13. Abd-Shukor, R., Kong, W.: J. Appl. Phys. **105**, 07E311 (2009)
14. Agail, A., Abd-Shukor, R.: Appl. Phys. A **112**, 501 (2013)
15. Yahya, N.A.A., Abd-Shukor, R.: Adv. Cond. Mat. Phys. **Article ID**, 821073 (2013)
16. Ozkaya, T., Baykal, A., Koseoğlu, Y., Kavas, H.: Cent. Eur. J. Chem. **7**, 410 (2009)
17. Jannah, A.N., Abdullah, H., Abd-Shukor, R.: Adv. Cond. Mat. Phys. **Article ID**, 498747 (2014)